ISSN 0010-5082, Combustion, Explosion, and Shock Waves, 2023, Vol. 59, No. 2, pp. 206–214. © Pleiades Publishing, Ltd., 2023.

Ignition Resistance of Wood Building Structures Exposed to a Firebrand Shower

D. P. Kasymov[a,*], M. V. Agafontsev[a], V. V. Perminov[a], E. L. Loboda[a], Yu. A. Loboda[a],V. V. Reino[b,], and K. E. Orlov[a]**

UDC 536.37

Published in *Fizika Goreniya i Vzryva*, Vol. 59, No. 2, pp. 91–100, March–April, 2023.
Original article submitted October 17, 2022; revision submitted October 17, 2022; accepted for publication December 14, 2022.

Abstract: The interaction of a firebrand shower with some types of combustible building materials and wood structures was studied experimentally. The heat flux generated by firebrands was determined, and the temperature fields of the most heat-stressed sections of the structures were analyzed. The heating rate of samples was estimated based on infrared thermography data. Under the selected experimental conditions, the bench sample was found to be the most resistant to ignition. Estimation of the near-surface temperature of the bench element showed that after 15-min continuous exposure to firebrands, the temperature in the zone of maximum accumulation of firebrands did not exceed 130°C. The wood fence model was found to be most prone to ignition (ignition delay time more than 15% lower compared to the other structures.

Keywords: wood, infrared diagnostics, fire resistance, heat flux, firebrands.

DOI: 10.1134/S0010508223020119

INTRODUCTION

Recently, there has been a global increase in the number of wildfires which spread to building zones with various infrastructure facilities, including residential buildings. These fires not only cause huge economic damage, but also endanger the life and health of people. Examples of such fires leading to catastrophic consequences and significant material damage are wildfires in Siberia and the Russian Far East in 2012 and 2019, Khakassia and Transbaikalia in 2015, the Irkutsk region and Yakutia in 2020–2021, Khanty–Mansi Autonomous Okrug in 2022, fires in Greece (2019), Portugal (2019), Australia (2019–2020), USA (California) (2018–2020), and Turkey (2021). In May 2022, more than 100 buildings and houses burned down in the Omsk region per day—due to storm wind, forest fire spread to the residential sector. The increase in the number of wildfires is associated, on the one hand, with the preference of people to live in forested areas, where the risk of fires is increased, and, on the other hand, with a lack of understanding of the mechanism of fire spread to urbanized areas. In addition, the regulations governing the construction and maintenance of buildings in forest areas needs to be improved in terms of fire safety. It is expected that the impact of such fires will increase sharply [1] as there is a fairly rapid increase in the number of residential buildings in the forest and forest-steppe zones [2]. In addition, global climate change increases the likelihood and intensity of forest fires [3], which, in turn, affects atmospheric and global climatic processes [4, 5].

In some cases, a decisive factor in the ignition of forest combustible materials and fire spread are firebrands [6, 7]. This process includes three important

[a]Tomsk State University, Tomsk, 634050 Russia;
*denkasymov@gmail.com.
[b]Zuev Institute of Atmospheric Optics, Siberian Branch, Russian Academy of Sciences, Tomsk, 634055 Russia;
**reyno@iao.ru.

steps: firebrand generation and transport and the ignition of combustible materials by firebrands. Many studies in this area have focused on firebrand transport whereas little attention has been paid to firebrand generation and the ignition of combustible materials by firebrands [8]. In addition, it is necessary to take into account the ignitability of certain building materials under exposure to a point source of heat, which will allow an improvement in existing fire-fighting technologies in construction.

Recent developments of firebrand generators and research conducted using these generators have significantly expanded knowledge in the field of assessing the vulnerability of structures in fire conditions [9, 10]. Recently, there has been extensive systematic research of firebrand generation, including full-scale investigations of the ignition of building structures [11] and modeling of the interaction of firebrands with wood structures [12]. In particular, the research has focused on evaluating the vulnerability of vents [13], roof elements [14], siding treatments, cornices [15], and structural elements of buildings and structures [16] for different environmental parameters and fire intensity.

At present, modern methods of infrared (IR) diagnostics are widely used to study combustion processes and wildfires [17–21]. Some recommendations for the use of thermography to test the fire resistance and fire hazard of wood and other building materials have been developed. This work requires additional experiments. IR diagnostics allows the evaluation of the dynamics of the true temperature field in laboratory and full-scale fire tests of elements of wood buildings and structures [22–24]. The development of a technique based on these data to test the fire resistance and fire hazard of wood building structures with the use of thermography will reduce the economic component of this kind of work and at the same time increase the efficiency of data acquisition, resolvability, and informativeness. It should be noted that the task does not only reduce to the practical aspects of fire protection of wood buildings and structures, but is also a reserve for improving the physicomathematical theory of wildfires, the understanding of the generation and transport of firebrands, and their potential in the ignition of combustible materials and initiation of spotted fires.

The aim of the work is physical modeling of the interaction of a firebrand shower with some types of combustible building materials and wood structures (a bench model, a compound fence, and an inside corner) with subsequent evaluation of their thermophysical parameters (temperature field, sample heating rate, heat fluxes, and ignition delay time).

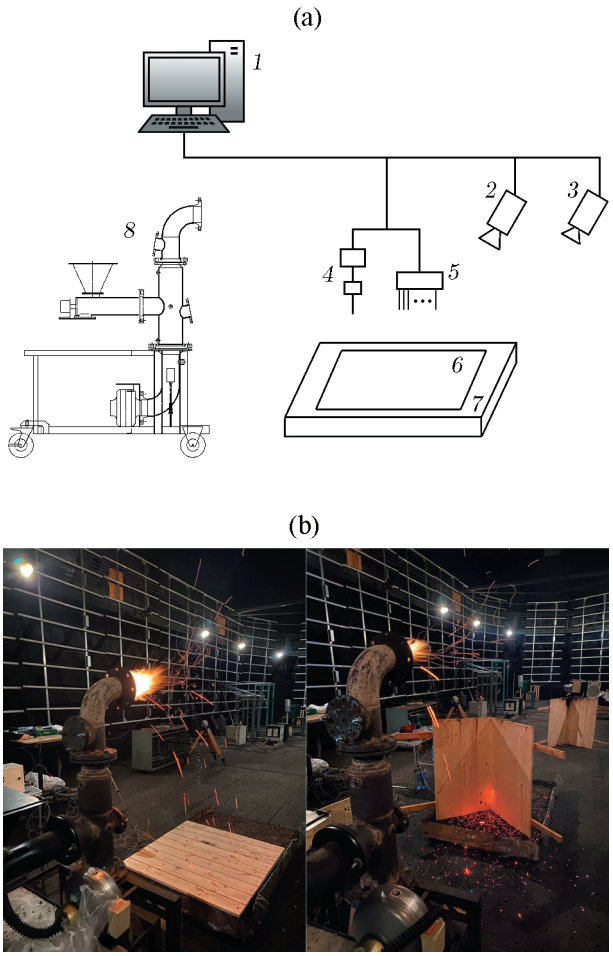

Fig. 1. Experimental site: diagram (a) and photographs from the experiment location (b): (*1*) personal computer; (*2*) JADE J530SB infrared camera; (*3*) Sony FDR X3000 video camera; (*4*, *5*) data acquisition system (thermocouple data acquisition unit; a SBG01 heat flux sensor with an AKIP-74824A oscilloscope); (*6*) wood structure (in this case; the bench model); (*7*) underlying surface in the form of a box with soil; (*8*) firebrand generator.

EQUIPMENT AND EXPERIMENTAL TECHNIQUE

The experiments were carried out in the large aerosol chamber of the Institute of Atmospheric Optics, Siberian Branch, Russian Academy of Sciences, which is part of the Center for Collective Use "Atmosphere." The volume of the chamber is 2000 m^3. The use of this chamber eliminates the effect of side and head wind, which is inevitably present in field experiments and affects the characteristics of flying particles.

Figure 1 shows the experimental site with equipment.

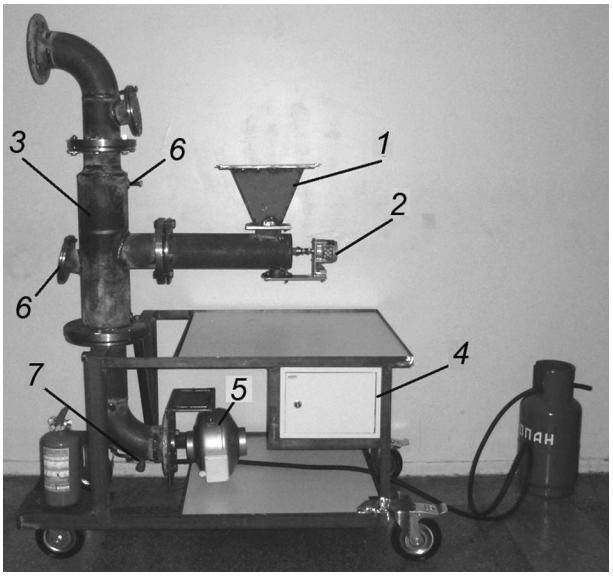

Fig. 2. General view of the firebrand generator: (*1*) receiving hopper; (*2*) screw feeder of firebrands; (*3*) furnace working area; (*4*) electric power cabinet; (*5*) TUBE 250XL duct fan; (*6*) measuring windows.

The experimental equipment included: a scientific JADE J530SB IR camera with a narrow-band optical filter with an operating wavelength of 2.5–2.7 μm for measuring temperature in the range 300–1500°C (the choice of which is due to the high radiation intensity of water vapor and carbon dioxide in the spectral range used) and a lens with a focal distance of 50 mm; Canon LEGRIA HF R86 (Canon Inc., China) and Sony FDR X3000 (Sony Group Corporation, China) camcorders for evaluating the ignition delay of samples of wood building materials and recording firebrand generation and transport; K-type thermocouples with a junction diameter of 200 μm for evaluating the temperature field near the surface of wood samples; a Hukseflux SBG01 heat flux sensor with an operating range of 0–100 kW/m^2; AKIP-74824A for recording thermoEMF; AND MX-50 (AND, Japan) moisture analyzer for controlling the moisture content of samples under study. The IR camera sensor size is 320×240 pixels, and the shooting speed is 7 fps. The distance from the outlet of the firebrand generator to the thermal imager is 1.7 m. The physical size of the area of IR camera measurements is 0.71×0.53 m.

The firebrand generator is equipped with a screw mechanism allowing for a long and continuous supply of combustible material, and provides for the creation of an air curtain to stop smoke for safer operation in confined spaces [25]. A photograph of the setup is shown in Fig. 2.

The operation of the setup results in firebrand transport under the action of air flow, firebrand ignition and generation into the environment with the option of adjusting the rate and volume of gas supply, air flow velocity, and the volume of firebrands.

The following pine building structures were selected as samples: a bench element, a compound fence, and an inside corner of a building (Fig. 3). Before the experiments, the moisture content of woo did not exceed 10%.

The firebrand shower occurring during forest fires was produced using wood pellets. The firebrand sizes were chosen in accordance with the data of full-scale experiments to simulate a ground fire in a pine forest [26, 27]. The wood pellets were 8 mm in diameter and 30–50 mm long.

In this study, the firebrand generator operated in the mode of periodic addition of pellets to the furnace area of the setup, which allowed both continuous and intermittent, with a given frequency, generation of firebrands.

The main control parameter was the surface temperature of the investigated wood structures and the magnitude of the heat flux.

The surface temperature of the bench sample was controlled using Chromel–Alumel thermocouples with a junction diameter of 500 μm. The surface of the bench sample was covered with a uniform network of thermocouples with a spacing of 10 cm. The layout of the sensors is shown in Fig. 4.

In the fence and inside corner samples, the heat flux sensor was placed in the middle of the sample at a height of 10 cm from the ground surface and flush mounted into the structure.

The experiment was carried out as follows. A model wood structure was mounted on an underlying surface which was a box with soil of natural origin. The structures were made of meter-long boards 0.14 m wide and 0.016 m thick and had the following dimensions: the bench was 1×1 m in size with the gap between the boards chosen based on the characteristic firebrand diameter, which did not exceed 8 mm; the compound fence was 1 m high and 1.1 m wide; the corner structure consisted of two identical sheets 1 m high and 0.62 m wide, attached to each other at an angle of 90°. Next, in the zone of the mounted sample, the process of firebrand generation, transport, and subsequent deposition was started (Fig. 5). For each type of building structures, at least three experiments were carried out.

A fire exposure was modeled in which flying firebrands accumulated in the surrounding area and on roof elements. Such a scenario is possible in massive crown fires near residential buildings in an urbanized area.

(a)

(b)

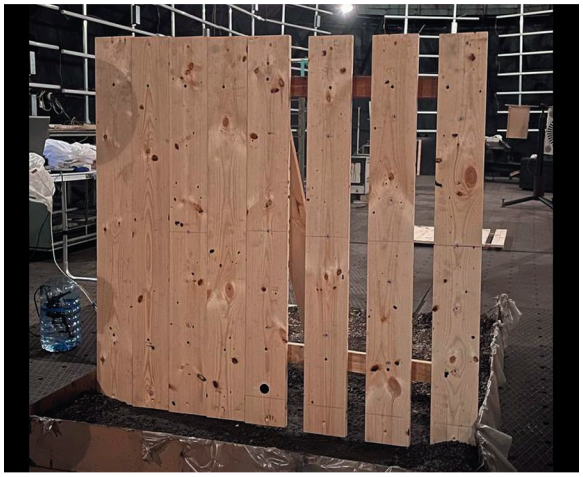

(c)

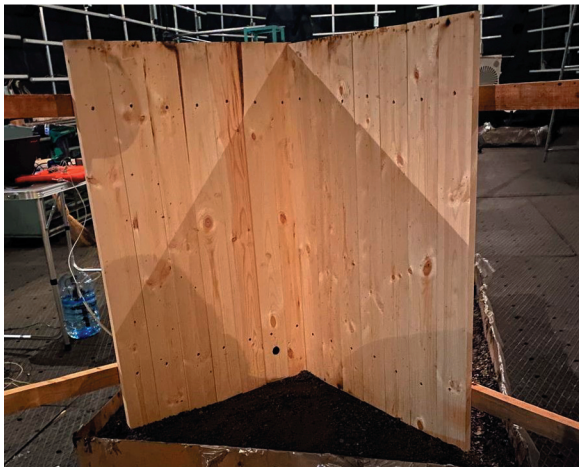

Fig. 3. Wood samples: (a) bench; (b) compound fence; (c) inside corner of a building.

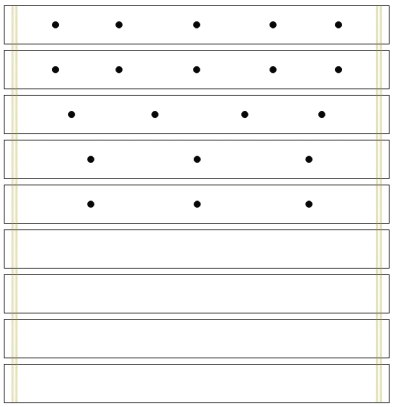

Fig. 4. Schematic arrangement of thermocouples in the bench sample.

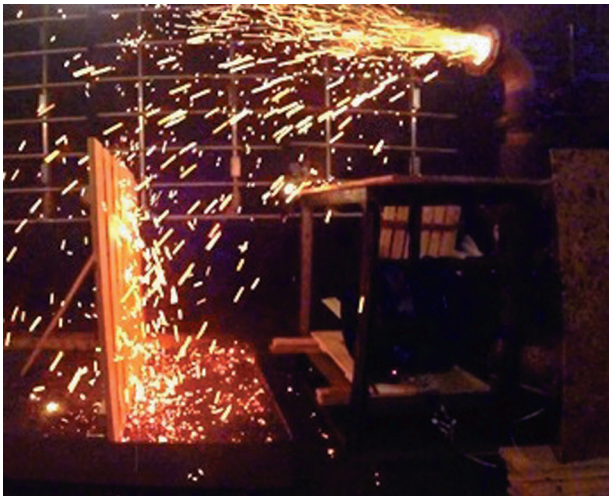

Fig. 5. Compound fence model used in the experiment.

RESULTS OF IR THERMOGRAPHY OF SAMPLES IN FIRE EXPERIMENTS

During the experiments, a series of IR images of the process of firebrand generation and interaction with wood structures was obtained (Fig. 6). Further data processing was carried out using the Altair software.

In the case of the corner structure and compound fence, falling firebrands accumulated near the structure (Fig. 6) and continued to interact with the wall surface. During long-term interaction, the total energy of firebrands is high enough to ignite these structures with subsequent combustion.

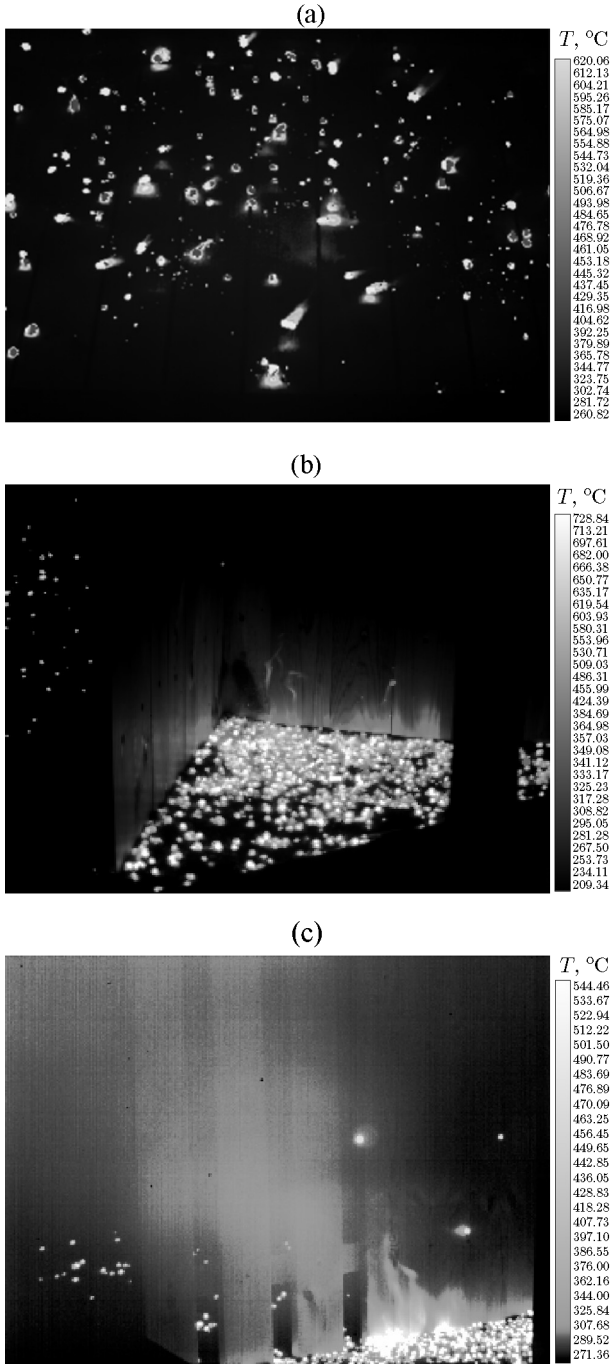

Fig. 6. Thermograms of the surface after exposure to a firebrand shower: (a) bench; (b) inside corner of a building; (c) compound fence.

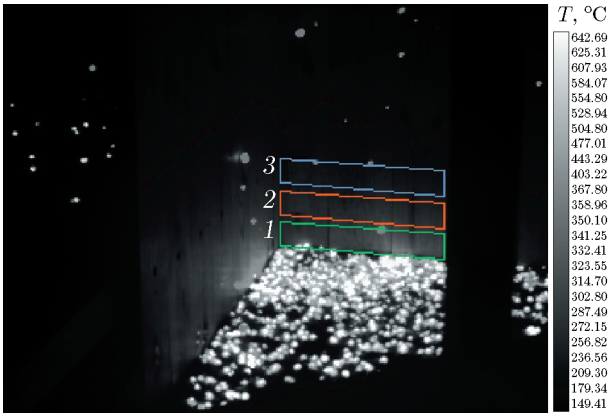

Fig. 7. Thermogram of the surface of the corner structure with the established measuring areas.

Based on the obtained thermograms, the firebrand temperature at the moment of the fall was within 490–650°C. At the moment of firebrand ejection from the generator, it was 750–800°C [28].

To analyze the change in temperature on the surface of the samples, the following processing was performed. In the Altair software workspace, three rectangular regions (Fig. 7) were selected that corresponded to the most heat-stressed regions of the sample surface, and the data from these regions were used to obtain the time dependence of the temperature averaged over the region. By averaging these temperature distributions over three regions, we obtained the temperature change on the surface of the test sample in the most heated zone (Fig. 8).

Analysis of the graphs in Fig. 8 leads to the conclusion that the fence structure is heated more intensely than the inside corner of a building. This can be explained by the fact that near the fence, the area of the region of accumulation of fallen firebrands is larger than in the inside corner. Furthermore, in the inside corner, the density of deposition of firebrands from the same region is definitely higher. As a result, the large number of fallen firebrands in a limited area prevents the access of the oxidizer to the lower layers.

MEASUREMENT WITH CONTACT SENSORS

The heating dynamics of the surface of the wood bench, was evaluated by analyzing thermocouple measurements. In the experiments, the bench was located in such a way that the main zone of falling firebrands was in the middle of the sample. The change in the maximum near-surface temperature was estimated (Fig. 9).

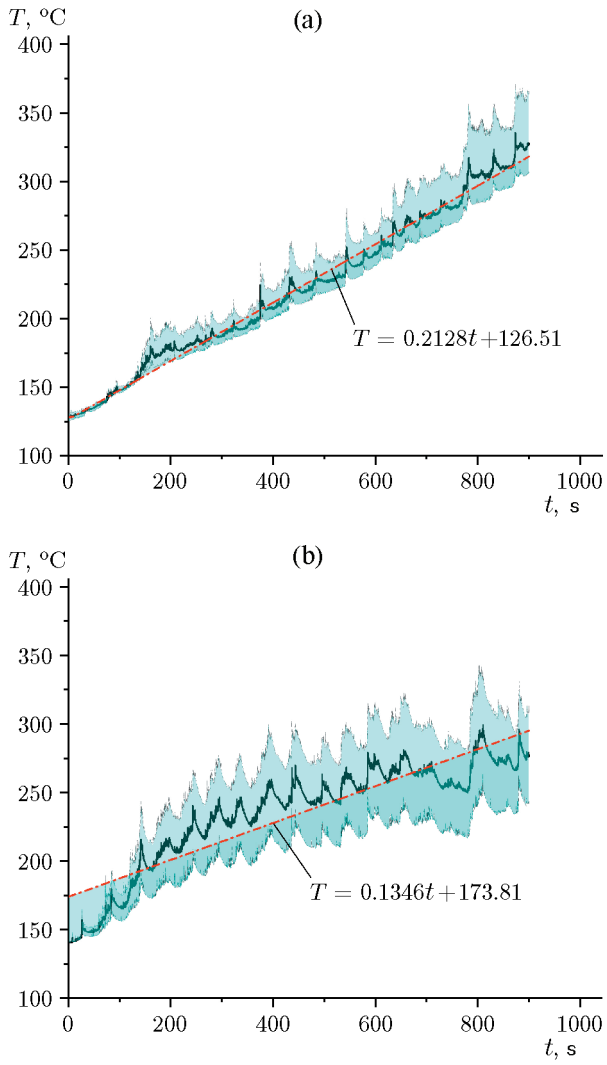

Fig. 8. Heating rate of the surfaces of the fence (a) and the inside corner of a wood structure (b).

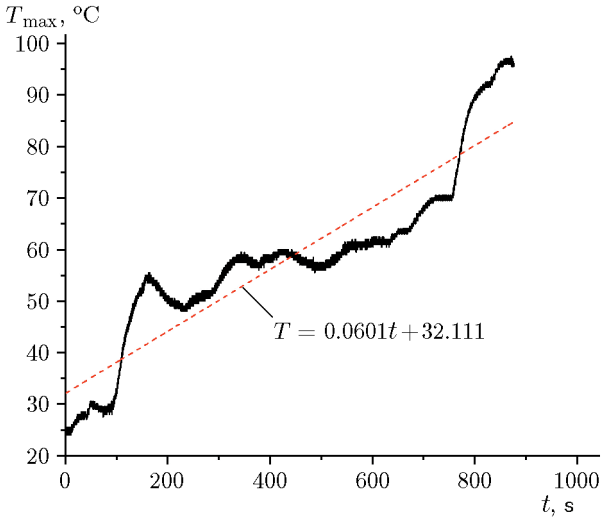

Fig. 9. Heating rate of the surface of the wood bench.

Comparing Figs. 8 and 9, we can conclude that the bench element is the least exposed to the heat from firebrands. Estimates of the time required for the start of wood pyrolysis [29] show that ignition of the bench element in the firebrand generation mode used will require at least 83 min, ignition of the corner element 37 min, and ignition of the fence element 24 min.

To estimate the energy characteristics of the firebrand shower, we studied the heat flux from a single firebrand. The nonlinear growth of the heating rate curve (see Fig. 9) is caused by the uneven generation of firebrands by the setup.

To measure the heat flux from a single firebrand, we used a heat flux sensor with a multilayered structure, which was calibrated according to an AChT 45/100/1100 reference emitter (Etalon company) with a temperature range of 573–1373 K. A single firebrand was placed in a metal container, where it was heated to smoldering combustion by a gas burner. Then the firebrand moved to the receiving surface of the vertically mounted heat flux sensor, whose signal was recorded by an analog-to-digital converter based on an ADS1115 chip and an ATmega328 microcontroller. For each firebrand size studied, 10 control measurements were carried out. The average values of the heat flux during firebrand smoldering are in the range 0.097–3.891 kW/m^2 (depending on the firebrand length).

Figure 10 shows the results of measuring the heat flux near the region of firebrand accumulation. The maximum values of the heat flux did not exceed 10 kW/m^2 for the compound fence element and 6 kW/m^2 for the inside corner of a building. The combustion of firebrands caused smoldering of wood, but no further combustion was observed. The heat flux data are consistent with the results of a study [30] of the probability of igniting a residential building model by a firebrand shower under similar conditions.

The present study was carried out in the absence of incident air flow, but for a detailed evaluation of the probability of igniting various structures by a point source of heat, it is required to take into account the presence of air flow of different velocity, which undoubtedly enhances the smoldering of firebrands. Laboratory studies have shown [31–33] that air flow in the firebrand accumulation zone can increase severalfold the probability of flame combustion of firebrands with subsequent spread of the fire to plant combustible materials and building structures.

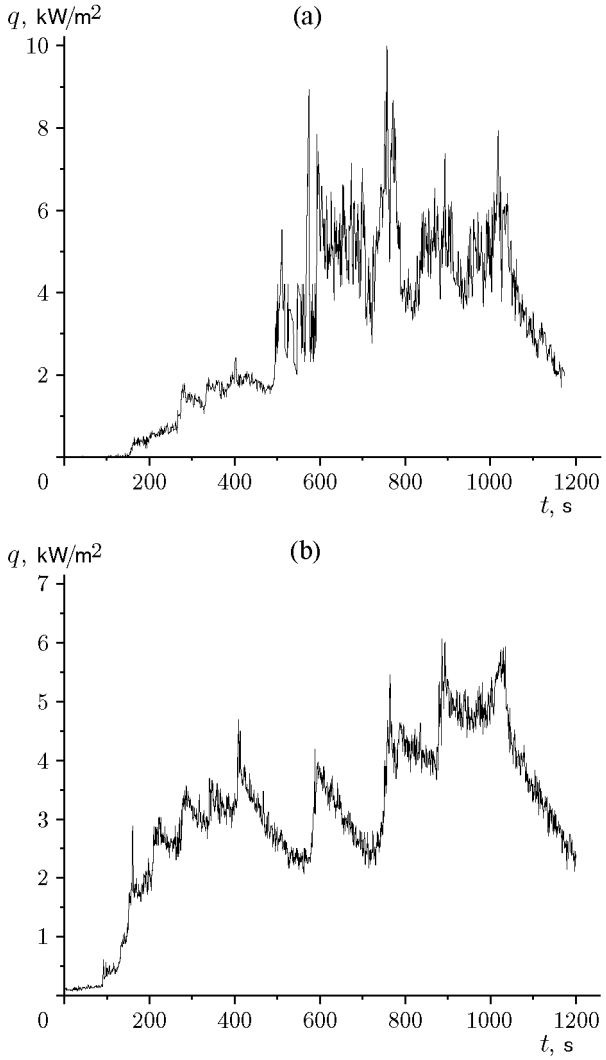

Fig. 10. Change in the heat flux incident on the surface of the compound fence (a) and the inside corner of a building (b) near the firebrand accumulation zone.

The heat flux for the bench element was not evaluated. This is due to the fact that smoldering firebrands falling on the control and measuring device will give obviously overestimated values of the heat flux due to the conductive component of heat transfer.

CONCLUSIONS

Integrated experimental studies were performed to investigate the impact of a model shower of firebrands of various configurations on some types of combustible building materials and wood structures (bench model, a compound fence with permeable and impermeable regions, inside corner of a building). A feature of the physical modeling of the firebrand shower in the present study was continuous firebrand generation for 15 min.

According to the results of analysis of the obtained thermograms, the temperature of firebrands at the moment of the fall was in the range 490–650°C. At the same time, at the moment of ejection from the generator nozzle, the temperature of burning firebrands was 750–800°C. The temperature distribution on the surfaces of the samples exposed to the firebrand shower was experimentally determined by the noncontact method of IR diagnostics. This made it possible to establish heat-stressed regions on the surface of models of wood structures under the impact of the ground forest fire front and estimate their characteristic sizes with high accuracy.

The heat flux generated by smoldering firebrands and the temperature field of the most heat-stressed regions of the structures under study were evaluated.

The sample heating rate was estimated from the data of IR thermography. The heating rate of the inside corner element averaged over three tests was 0.21°C/s, and for the fence element, it was 0.13°C/s. The difference in the heat flux and heating rates for the fence and inside corner elements is due to the fact that the heating of the second structure is more intense because of the larger area of firebrand accumulation in front of the investigated sample.

For the selected experimental conditions, the bench sample turned out to be resistant to ignition. Estimation of the near-surface temperature of the bench element showed that after 15-min continuous exposure to firebrands, the temperature in the zone of maximum accumulation of firebrands did not exceeded 130°C. It should be noted that this low temperature in the central spot of the region of the fall of smoldering firebrands is insufficient for stable ignition of the structure.

The wood fence model was the most prone to ignition; the characteristic time of its ignition was 760 s. This is 8% lower compared to the other structures. The geometry of the inside solid angle in the experiment played the role of a barrier from which firebrands ricocheted, resulting in a decrease in the probability of their accumulation directly near the structure.

This study expands existing information on the fire resistance of wood building structures (bench model, a compound fence, and an inside corner) upon exposure to firebrands in large-scale fires.

The study was supported by the Russian Science Foundation (Project No. 20-71-10068; https://rscf.ru/en/project/20-71-10068/).

The results were reported at the 2nd International Conference “Physics and Chemistry of Combustion and Processes in Extreme Environments,” July 12–16, 2022, Samara.

REFERENCES

1. E. I. Foote, S. L. Manzello, and J. Liu, "Characterizing Firebrand Exposure during Wildland–Urban Interface Fires," in *Proc. Fire Mater. Conf. 2011*, pp. 479–491.
2. R. B. Hammer, V. C. Radeloff, J. S. Fried, and S. I. Stewart, "Wildland Urban Interface Housing Growth during the 1990s in California, Oregon, and Washington," Int. J. Wildland Fire **16** (3), 255–265 (2007); DOI: 10.1071/WF05077.
3. M. D. Flannigan, B. J. Stocks, and B. M. Wotton, "Climate Change and Forest Fires," Sci. Total Environ. **262** (3), 221–229 (2000); DOI: 10.1016/S0048-9697(00)00524-6.
4. E. Loboda, D. Kasymov, M. Agafontsev, V. Reyno, Y. Gordeev V. Tarakanova, P. Martynov, Y. Loboda, K. Orlov, and K. Savin, et al., "Effect of Small-Scale Wildfires on the Air Parameters near the Burning Centers," Atmosphere **12** (1) (2021), Article Number 75; DOI: 10.3390/atmos12010075.
5. S. L. Manzello, T. G. Cleary, J. R. Shields, A. Maranghides, W. Mell, and J. C. Yang, "Experimental Investigation of Firebrands: Generation and Ignition of Fuel Beds," Fire Saf. J. **43** (3), 226–233 (2008); DOI: 10.1016/j.firesaf.2006.06.010.
6. V. A. Perminov and V. I. Marzaeva, "Mathematical Modeling of Crown Forest Fire Spread in the Presence of Fire Breaks and Barriers of Finite Size," Fiz. Goreniya Vzryva **56** (3), 94–105 (2020) [Combust., Expl., Shock Waves **56** (3), 332–343 (2020); https://doi.org/10.1134/S0010508220030107].
7. A. M. Grishin, A. D. Gruzin, and V. G. Zverev, "Heat and Mass Transport and the Propagation of Burning Particles in the Surface Layer of the Atmosphere during Upstream Forest Fires," Fiz. Goreniya Vzryva **17** (4), 78–84 (1981) [Combust., Expl., Shock Waves **17** (4), 418–423 (1981); https://doi.org/10.1007/BF00761211].
8. A. C. Fernandez-Pello, "Wildland Fire Spot Ignition by Sparks and Firebrands," Fire Saf. J. **91**, 2–10 (2017); DOI: 10.1016/j.firesaf.2017.04.040.
9. S. L. Manzello, "Summary of Workshop on Global Overview of Large Outdoor Fire Standards," NIST Special Publ. **1235** (2019); DOI: 10.6028/NIST.SP.1235.
10. S. Nazare, I. Leventon, and R. Davis, "Ignitibility of Structural Wood Products Exposed to Embers during Wildland Fires: a Review of Literature," Tech. Note No. 2153 (Nat. Inst. of Stand. and Technol., 2001); DOI: 10.6028/NIST.TN.2153.
11. S. Suzuki and S. L. Manzello, "Ignition Vulnerabilities of Combustibles around Houses to Firebrand Showers: Further Comparison of Experiments," Sustainability **13** (4), 2136 (2021); DOI: 10.3390/su13042136.
12. O. V. Matvienko, D. P. Kasymov, E. L. Loboda, A. V. Lutsenko, and O. I. Daneyko, "Modeling of Wood Surface Ignition by Wildland Firebrands," Fire **5** (2) (2022), Article No. 38; DOI: 10.3390/fire5020038.
13. S. L. Manzello, S. H. Park, J. R. Shields, Y. Hayashi, and S. Suzuki, "Comparison Testing Protocol for Firebrand Penetration through Building Vents: Summary of BRI/NIST Full Scale and NIST Reduced Scale Results," Report No. 1659 (NIST TN, 2010).
14. S. L. Manzello, Y. Hayashi, T. Yoneki, and Y. Yamamoto, "Quantifying the Vulnerabilities of Ceramic Tile Roofing Assemblies to Ignition during a Firebrand Attack," Fire Saf. J. **45** (1), 35–43 (2010); DOI: 10.1016/j.firesaf.2009.09.002.
15. S. L. Manzello, S. Suzuki, and Y. Hayashi, "Exposing Siding Treatments, Walls Fitted with Eaves, and Glazing Assemblies to Firebrand Showers," Fire Saf. J. **50**, 25–34 (2012); DOI: 10.1016/j.firesaf.2012.01.006.
16. S. L. Manzello and S. Suzuki, "Exposing Decking Assemblies to Continuous Wind-Driven Firebrand Showers," in *Proc. of the 11th Int. Symp. on Fire Safety Science* (2014); http://www.nist.gov/customcf/get_pdf.cfm?pub_id=913383.
17. S. Suzuki, A. Brown, S. L. Manzello, J. Suzuki, and Y. Hayashi, "Firebrands Generated from a Full-Scale Structure Burning under Well-Controlled Laboratory Conditions," Fire Saf. J. **63**, 43–51 (2014); DOI: 10.1016/j.firesaf.2013.11.008.
18. B. P. Vavilov, *Infrared Thermography and Thermal Control* (Spektr, Moscow, 2009) [in Russian].
19. J. J. O'Brien, E. L. Loudermilk, B. Hornsby, A. T. Hudak, B. C. Bright, M. B. Dickinson, J. K. Hiers, C. Teske, and R. D. Ottmar, "High-Resolution Infrared Thermography for Capturing Wildland Fire Behaviour: RxCADRE 2012," Int. J. Wildland Fire **25** (1), 62–75 (2016); DOI: 10.1071/WF14165.
20. O. Rios, E. Pastor, M. M. Valero, and E. Planas, "Short-Term Fire Front Spread Prediction Using Inverse Modeling and Airborne Infrared Images," Int. J. Wildland Fire **25** (10), 1033–1047 (2016); DOI: 10.1071/WF16031.
21. P. Sofan, D. Bruce, E. Jones, and J. Marsden, "Detecting Peatland Combustion Using Shortwave and Thermal Infrared Landsat-8 Data," Adv. Forest Fire Res., pp. 969–979 (2018); DOI: 10.14195/978-989-26-16-506_106.
22. M. M. Valero, D. Jimenez, B. Butler, C. Mata, O. Rios, E. Pastor, and E. Planas, "On the Use of Compact Thermal Cameras for Quantitative Wildfire Monitoring," Adv. Forest Fire Res. pp. 1077–1086 (2018); DOI: 10.14195/978-989-26-16-506_119.
23. A. M. Grishin, A. I. Filkov, E. L. Loboda, V. V. Reyno, A. V. Kozlov, V. T. Kuznetsov, D. P. Kasymov, S. M. Andreyuk, A. I. Ivanov, and N. D. Stolyarchuk, "A Field Experiment on Grass Fire Effects on Wooden Constructions and Pest Layer Ignition," Int. J. Wildland Fire **23** (3), 445–449 (2014); DOI: 10.1071/WF12069.

24. I. Vermesi, M. J. Di Domizio, F. Richter, E. J. Weckman, and G. Rein, "Pyrolysis and Spontaneous Ignition of Wood under Transient Irradiation: Experiments and A-Priori Predictions," Fire Saf. J. **91**, 218–225 (2017); DOI: 10.1016/j.firesaf.2017.03.081.
25. D. P. Kasymov, V. V. Perminov, A. I. Filkov, M. V. Agafontsev, V. V. Reino, E. L. Loboda, "Firebrand Generator for Poorly Ventilated Rooms," RF Patent No. RU 199698 U1, Appl. June 22, 2020; Publ. September 15.2020.
26. A. Filkov, S. Prohanov, E. Mueller, D. Kasymov, P. Martynov, M. El Houssami, J. Thomas, N. Skowronski, B. Butler, M. Gallagher, K. Clark, W. Mell, R. Kremens, R. M. Hadden, and A. Simeoni, "Investigation of Firebrand Production during Prescribed Fires Conducted in a Pine Forest," Proc. Combust. Inst. **36** (2), 3263–3270 (2017); DOI: 10.1016/j.proci.2016.06.125.
27. M. El Houssami, E. Mueller, A. Filkov, J. C. Thomas, N. Skowronski, M. R. Gallagher, K. Clark, R. Kremens, and A. Simeoni, "Experimental Procedures Characterising Firebrand Generation in Wildland Fires," Fire Technol. **52** (3), 731–751 (2016); DOI: 10.1007/s10694-015-0492-z.
28. S. Prohanov, A. Filkov, D. Kasymov, M. Agafontsev, and V. Reyno, "Determination of Firebrand Characteristics Using Thermal Videos," Fire **3** (4) (2020), Article No. 68; DOI: 10.3390/fire3040068.
29. D. Kasymov, M. Agafontsev, V. Perminov, P. Martynov, V. Reyno, and E. Loboda, "Experimental Investigation of the Effect of Heat Flux on the Fire Behavior of Engineered Wood Samples," Fire **3** (4) (2020), Article No. 61; DOI: 10.3390/fire3040061.
30. S. L. Quarles and C. D. Standohar-Alfano, "Ignition Potential of Decks Subjected to an Ember Exposure," Tech. Report of Insurance Inst. for Business and Home Safety; https://ibhs.org/wildfire/ignition-potential-of- decks-subjected-to-an-ember-exposure/.
31. D. P. Kasymov, V. A. Tarakanova, P. S. Martynov, and M. V. Agafontsev, "Studying Firebrands Interaction with Flat Surface of Various Wood Construction Materials in Laboratory Conditions," J. Phys.: Conf. Ser. **1359**, 012092 (2019); DOI: 10.1088/1742-6596/1359/1/012092.
32. D. P. Kasymov, M. V. Agafontsev, V. A. Tarakanova, E. L. Loboda, P. S. Martynov, K. E. Orlov, and V. V. Reyno, "Effect of Wood Structure Geometry during Firebrand Generation in Laboratory Scale and Semi-Field Experiments," J. Phys.: Conf. Ser. 1867, 012020 (2021); DOI: 10.1088/1742-6596/1867/1/012020.
33. V. A. Tarakanova, D. P. Kasymov, O. V. Galtseva, and N. V. Chicherina, "Experimental Characterization of Firebrand Ignition of Some Wood Building Materials, " Bull. Karaganda Univ. Phys., Ser. No. 4 (100), 14–21 (2020); DOI: 10.31489/2020Ph4/14-21.